JOURNAL OF PROPULSION AND POWER
Vol. 12, No. 6, November–December 1996

# Interior Plasma Diagnostics of Arcjet Thrusters

Mark A. Cappelli* and P. Victor Storm†
*Stanford University, Stanford, California 94305-3032*

**We review past experimental measurements of internal flow properties of arcjet thrusters. These measurements are generally classified as either intrusive, requiring design changes to prototype thrusters, or nonintrusive, and include measurements of cathode temperature, as well as static pressure, flow temperatures (vibrational, rotational, electronic, translational), electron density, and velocity throughout the interior region extending to the exit plane. Comparisons are made to available model predictions. These measurements, performed on a wide range of thrusters, and operating on variety of propellants, indicate that the nozzle plasma flow may be removed from local thermodynamic equilibrium.**

## Nomenclature

$\ell n\,\Lambda$ = coulomb logarithm
$\dot{m}$ = propellant mass flow rate, kg $s^{-1}$
$n_e$ = electron number density, $m^{-3}$
$P$ = arcjet power, W
$p_{stag}$ = stagnation pressure, Pa
$p_{throat}$ = throat static pressure, Pa
$T_{cat}$ = cathode temperature, K
$T_e$ = electron translational temperature, K
$T_{elec}$ = electronic excitation temperature, K
$T_{rot}$ = rotational excitation temperature, K
$T_{tran}$ = heavy species translational temperature, K
$T_{vib}$ = vibrational excitation temperature, K
$\sigma_{SH}$ = Sptizer–Harms electrical conductivity, $\Omega^{-1}$ $m^{-1}$

## I. Introduction

ARCJET propulsion systems have been successfully employed in stationkeeping applications. To enable other applications such as repositioning or orbit transfer, the arcjet must deliver 1000 s of specific impulse at 35–50% thrust efficiency.[1] However, efficiencies approaching 50% at high specific impulse have not yet been achieved. The future design of more efficient and reliable thrusters requires a better understanding of the physical processes governing arcjet operation. This understanding can be obtained through a combination of experimental diagnostics and analytical modeling. Many studies have been conducted to investigate arcjet performance under different operating conditions, electrical configurations, and geometries.[2] Understanding the physical processes governing the arcjet operation requires a detailed knowledge of the plasma properties everywhere in the flowfield. A great deal of research has been conducted to measure the flow properties in the plume of arcjet thrusters using electrical and optical techniques.[2–4] Much of this work was driven by the need to understand the effect that the partially ionized and chemically reacting plume may have on other spacecraft surfaces and communications. As far back as the early sixties,[5] mass flux probes, impact probes, and enthalpy probes were implemented as exit plane and plume diagnostics to better understand the performance of these devices. More recently, advanced optical diagnostics[6–9] have been developed and implemented to measure the exit plane flow properties and to better understand the thermal and chemical nonequilibrium nature of arcjet flows. Although much has been learned from these exit plane studies, it is evident that little is known about the plasma properties within the constrictor region and nozzle of the arcjet, yet it is here where the plasma behavior controls the arcjet performance.

In this article, we will review some past measurements made by other researchers and our own recent measurements of flow properties in the nozzle interior and constrictor (near-cathode) region of arcjet thrusters. These measurements can be classified as either intrusive or nonintrusive, depending on whether significant changes were made to the arcjet thruster to carry out the diagnostic. The intrusive measurements reviewed here include the static pressure measurements in both low-power (1-kW) thrusters using simulated hydrazine decomposition products as a propellant[10]; static pressure measurements in high-power (30-kW) thrusters operating with nitrogen as a propellant[11]; current distribution and floating potential measurements conducted using a segmented anode configuration in a 1-kW arcjet[12]; spectroscopic emission measurements of $n_e$ and characteristic temperatures for $T_{vib}$, $T_{elec}$, and $T_{rot}$ in the expansion nozzle of 1-kW thrusters using simulated hydrazine decomposition products as a propellant[13]; similar measurements to those described in Ref. 13 in 26-kW thrusters using ammonia as a propellant[14]; spectroscopic imaging of $T_e$ and $T_{elec}$ in a medium-power, water-cooled thruster using hydrogen as a propellant[15]; and $n_e$ and $T_{elec}$ in the constrictor region of a low power (1–3-kW) arcjet operating with helium as the propellant.[16] The nonintrusive measurements reviewed here include spectroscopic emission measurements of the near-cathode region $n_e$ and $T_{cat}$ in low and medium power (1- and 5-kW, respectively) hydrogen arcjet thrusters[17,18]; and laser-induced fluorescence (LIF) measurements of velocities in the nozzle of a low-power hydrogen arcjet thruster.[19] Despite the variations in propellant and differences in operating conditions, there are many common features in flow behavior associated with the various thrusters studied, some of which are discussed in the following sections.

## II. Static Pressure Measurements

Static pressure measurements are useful in interpreting internal flow behavior in arcjets. In many cases, they can provide insight into the losses associated with nonideal or viscous effects. In general, static pressure measurements reflect changes in the flowfield characteristics, which are expected to influence arcjet thruster performance and stability.[20]

Harris et al.[11] presented a detailed study of the static pressure variation in a 30-kW water-cooled arcjet thruster operating with nitrogen as a propellant. In that study, the arcjet was

Received Nov. 2, 1994; revision received Feb. 15, 1996; accepted for publication Aug. 17, 1996. 

*Associate Professor, High Temperature Gasdynamics Laboratory. Member AIAA.

†Research Assistant, High Temperature Gasdynamics Laboratory. Student Member AIAA.

instrumented with 16 equally spaced pressure taps located in positions ranging from the arcjet plenum, through an extended constrictor, nearly to the exit plane of the nozzle. Such measurements can be classified as intrusive, in that it is not clear how the presence of such features may perturb or alter the internal flow characteristics. It is useful to examine here, nonetheless, some of the conclusions drawn from that study.

An arcjet flow, such as that investigated by Harris et al.,[11] is expected to be far removed from ideal isentropic conditions, and will experience imperfect gas effects. Despite this, it is interesting to note that the ratio of axial static pressure to stagnation pressure (taken to be the pressure measured by the upstream tap in the plenum) is independent of $\dot{m}$ or $P$ as expected from a quasi-one-dimensional analysis, if the entire nozzle flow is choked. For all arc powers and flow rates studied, their measurements further indicated that the sonic point was located beyond the end of the constrictor, suggesting that viscous boundary-layer growth is significant within the constrictor. Up to the sonic point, an ideal quasi-one-dimensional analysis would indicate that the static pressure should increase with the square root of temperature (for a constant $\dot{m}$), reflecting the drop in density with temperature and the choked condition at the sonic point. If the radial pressure gradients are small, then assuming that the plasma is significantly ionized in the arc core, $n_e$ is expected to decrease with the square root of the temperature. As is discussed later, recent measurements do not reflect this trend, strongly indicating a departure from ideal conditions.

Similar measurements have been performed by Talley et al.[10] in a 1-kW laboratory arcjet thruster operating on mixtures of hydrogen and nitrogen to simulate hydrazine decomposition products.[10] In their facility, five pressure taps were machined into the anode housing, providing static pressure measurements at locations of approximately 1.5 mm upstream of the throat, at the throat, and three measurements distributed along the expansion nozzle. Unlike the 30-kW arcjet of Harris et al.,[11] there is no significant constrictor channel in these low-power devices, and so it is more likely that the sonic point will coincide with the location of the throat. This is supported by the critical pressure ratio (ratio of static pressure to $p_{stag}$ under choked conditions) of 0.52 measured in the throat for the arc-ignited low-power thruster,[10] unlike the 0.66–0.9 values measured in the constrictor region of the arc-ignited high-power thrusters.[11] Talley et al.[10] report, however, that their cold-flow $p_{throat}$ is significantly greater than the critical pressure ratio, indicating that the sonic point under cold-flow conditions has moved downstream of the throat. They attribute this behavior to the strong swirl component of velocity in the cold-flow case that is dampened out following arc ignition.

The throat static pressure measurements of Talley et al.[10] combined with an estimate of the temperature in the arc core of 20,000–40,000 K (not atypical for a constricted arc at high pressures), allow an estimate of $n_e$ in the core of the arc near the arcjet throat, provided we assume that the arc is in local thermodynamic equilibrium. Using the static pressure measurements of Ref. 10 (measured near the converging section of the nozzle), which range from 20–50 psia for $\dot{m}$ = 35–65 mg/s ($P/\dot{m}$ of 10–30 MJ/kg), and taking $p_{throat}/p_{stag} \sim 0.52$, we estimate throat electron number densities ranging from $6 \times 10^{22}$–$3 \times 10^{23}$ m$^{-3}$. Recently, Zube and Myers[13] measured $n_e$ from Stark broadening of hydrogen spectral lines in the upstream region of the expansion nozzle of a nearly identical arcjet thruster, also operating on simulated hydrazine decomposition products, over a comparable range of $P/\dot{m}$, albeit at much higher $\dot{m}$ (100 mg/s). Despite these different operating conditions, a comparison of the calculated $n_e$ to the measurements of Zube and Myers,[13] reported at a distance of 3 mm downstream of the throat ($\sim 10^{21}$ m$^{-3}$), indicates that significant axial gradients in $n_e$ exist in the near vicinity of the cathode and throat. Indeed, very strong axial number densities were measured near the throat of a 26-kW ammonia arcjet by Hargus et al.,[14] using spectroscopic methods similar to those of Zube and Myers.[13] We speculate that such strong axial gradients in $n_e$ contribute to the stability of a diffuse arc attachment at the anode in this region of the nozzle. A lower $n_e$ and cooler plasma will result in a correspondingly lower current density for a given electric field strength. A transition from a diffuse to constricted arc attachment at the anode has been shown to be less favorable at lower attachment current densities.[21,22]

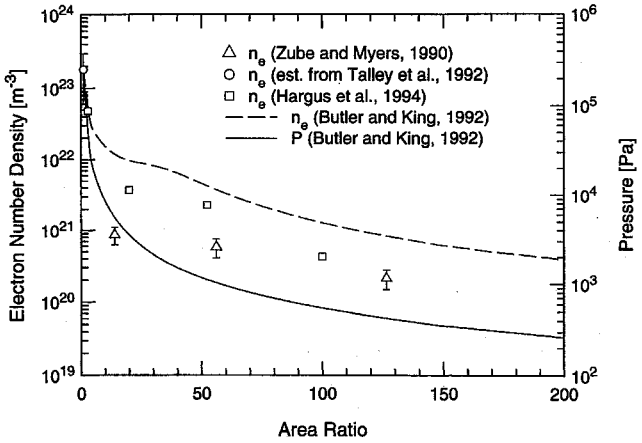


**Fig. 1 Axial variation in $n_e$ in a 1-kW class arcjet. The solid and dashed lines are the calculations for a low-power arcjet of Butler and King,[20,23] (see, e.g., Ref. 17) with hydrogen as a propellant. The data points are for a low-power thruster operating on hydrazine decomposition products from Ref. 13 (triangles), a high-power thruster operating on ammonia from Ref. 14 (squares), and, as estimated in the text, from the static pressure measurements of Ref. 10 (circles).**

The strong axial variation in $n_e$ in low-power arcjet thrusters has been captured by recent single-fluid magnetohydrodynamic (MHD) models developed by Butler and King.[20,23] In Fig. 1, we graph the model simulations for a (nominal) 1-kW arcjet thruster operating with hydrogen as a propellant ($\dot{m}$ = 13.1 mg/s and $P/\dot{m}$ = 115 MJ/kg), as well as available experimental data.[10,13,14] Although the results of Refs. 10 and 13 are for an entirely different propellant, and the results presented in Ref. 14 are for much higher powers, we include them on the graph for illustrative purposes. We see that in the hydrogen arcjet thruster, the predicted axial variation in $n_e$ is in qualitative agreement with the observations in essentially the same thruster operating on simulated hydrazine decomposition products, and with the measurements made in the 26-kW ammonia engine.

## III. Electrical Measurements

Until the recent electrical studies of Curran and Manzella,[12] we could only speculate as to the mode and distribution of current attachment along the anode surface in low-power arcjets. In that study, an arcjet of identical geometry to those baselined for use in communications satellites was instrumented with a segmented anode. Although inherently an intrusive diagnostic, this segmented anode design allowed them to estimate the current distribution and floating (plasma) potential as well as the anode fall voltage. In addition, they were able to perturb the attachment (i.e., electrically isolate various segments) to force current to a particular region along the anode.

The anode described in Ref. 12 was divided into five segments. The first consisted of the converging section up to the end of the constrictor/throat. The second, third, and fourth sections were centered approximately 1, 2.5, and 4 mm downstream of the throat, respectively. The last segment consisted of the remaining section of the nozzle. Each segment was separated from the others by thin boron–nitride spacers.

The most interesting finding is that under normal operation (all segments connected together and connected to the power supply) the current was nearly equally distributed to all but the first segment (which collected little or no current under steady operation). This finding indicates that the current density decreases significantly along the axial direction, consistent with the measured drop in $n_e$.[13] The first segment, when electrically isolated, barely influenced the current attachment at the remaining four segments. This is an important result, in that it indicates that little or no current is collected by this region of the anode. Although the floating potential of this segment was not measured while all others were connected, it was found to be approximately 35 V (relative to the cathode) when the current was forced to the fifth segment.[12] Using 35 V as an estimate of the voltage between the cathode and the end of the constrictor (which is approximately 0.75–1.0 mm from the cathode tip, depending on the gap spacing), we can estimate the extent of arc constriction (arc diameter). To do this, we need the electrical conductivity, which, if the arc core is fully ionized, is given by the Spitzer-Harm expression[24] (in MKS units):

$$\sigma_{SH} = 1.53 \times 10^{-2}(T_e^{3/2}/\ell n\ \Lambda) \qquad (1)$$

Here, $\ell n\ \Lambda$ depends (weakly) on both $n_e$ and $T_e$. If we assume $T_e$ = 30,000 K, $n_e = 10^{23}$ m$^{-3}$, and that the arc core is highly ionized, we estimate the electrical conductivity to be approximately 16,000 $\Omega^{-1}$ m$^{-1}$. Using a current of 11A, we arrive at an arc diameter of approximately 200 $\mu$m. Comparing this to the constrictor diameter of approximately 700 $\mu$m indicates that the arc is constricted to about 10% of the throat area. This estimate is within a factor of 2 of what has been measured based on Stark broadened axial line emission from a 1-kW arcjet operating on hydrogen.[17]

Another interesting result of the Curran and Manzella study[12] is that when the last segment is isolated from the power supply (and its current is shifted to the next upstream segment), the voltage on the last segment can be used to estimate the anode fall voltage at the next upstream segment. It is found that when isolated, the voltage of the fifth segment (relative to the cathode) was roughly equal to the voltage on all of the remaining connected segments. If we can assume that this last segment acts as an emissive probe, then it will measure the local plasma potential. This suggests that the anode fall voltage in the distant nozzle may be negligible. This result is not surprising if one considers that the field near the anode consists of both a resistive component balanced by an ambipolar component that is associated with gradients in plasma density:

$$E \approx (J/\sigma) - (kT/e)(\nabla n_e/n_e) \qquad (2)$$

We see that, at sufficiently low current densities, the plasma potential can in fact be greater than the anode potential (giving rise to a negative fall). In the case at hand, it appears that the current densities are sufficiently low near the end of the nozzle that the anode fall is small. Another interesting experiment described in the study of Curran and Manzella[12] involved forcing the current to attach to the first (furthest upstream) segment by isolating the remaining four. The floating potential of the remaining four segments, when compared to the potential difference between the cathode and the first segment, affords an estimate of the anode fall voltage at the first segment. Under these conditions, a high current density ensues and we would therefore expect the anode fall to increase significantly. Indeed this was the case,[12] with the anode fall voltage increasing to approximately 40 V.

## IV. Optical Emission Measurements

Much has been learned about the internal flow characteristics of arcjet thrusters by studying the intrinsic plasma emission. One of the first and most thorough investigations of the nozzle flow of a prototype thruster was performed by Zube and Myers[13] using optical emission spectroscopy. In that study, a set of holes were drilled into the anode (nozzle) of a 1-kW arcjet thruster at three axial positions, approximately 3, 6, and 9 mm from the throat of a nozzle that had a maximum area ratio of 225:1. A set of holes were also drilled at various radial positions, approximately 9 mm from the throat of a nozzle similar to that described earlier, and at 9 and 12 mm from the throat of a nozzle of equal half-angle (30 deg), but extended to an area ratio of 400:1. Like the static pressure measurements, these measurements can be considered to be intrusive, in that it is not clear how the presence of such holes perturb or alter the internal flow characteristics. The research presented in Ref. 13 was motivated by the need to better understand the nonequilibrium processes in the nozzle of an arcjet thruster operating on mixtures of hydrogen and nitrogen to simulate hydrazine decomposition products. These nonequilibrium processes include vibrational, rotational, and electronic excitation, as well as finite rate recombination. Hargus et al.[14] extended the Zube and Myers spectroscopic method[13] to the study of a 26-kW ammonia arcjet thruster. Optical access holes were drilled into the sides of the nozzle at distances of 2.5, 12.7, and 22.9 mm downstream of the 2.5-mm constrictor. Their nozzle had an area ratio of 100:1 and a half-angle of 19 deg. The electron number density was measured from the line-of-sight-integrated spectral (primarily Stark broadened) linewidth of the $H_\beta$ transition in atomic hydrogen. Their measured axial variation in $n_e$ is compared to single-fluid calculations for the 1-kW arcjet (albeit at slightly different operating conditions and for hydrogen as a propellant) in Fig. 1. The differences between model predictions and measurements are within a factor of 2–10, and might be accounted for by the slight differences in operating conditions.

An interesting result of the Zube and Myers study[13] is that extending the nozzle clearly perturbs the upstream current and plasma properties. They found that the $n_e$ that was measured 9 mm from the throat of an arcjet, having a 12-mm-long nozzle, was significantly less (by some 40% or so) than that at the same location in an extended nozzle (15 mm) of equal expansion angle. This result reveals the influence that the nozzle geometry may have on arc behavior. More importantly, it suggests that a nonnegligible fraction of the current extends down into the low-density region of the flow, consistent with the electrical measurements and findings of Curran and Manzella.[12]

Their measured $T_{elec}$ (from the Balmer transition series of atomic hydrogen), $T_{rot}$ and $T_{vib}$ (from the $C^3\Pi_u - B^3\Pi_g$ electronic transition of molecular nitrogen) are displayed in Fig. 2. Also displayed in the figure is the translational temperature computed using the arcjet model of King and Butler[20,23] (see for example Ref. 17) for a similar low-power arcjet operating on hydrogen. Like $n_e$, the temperatures drop in the expansion zone (beyond an area ratio of about 10), most noticeably for $T_{elec}$, which is argued to be close to $T_e$ because of rapid thermalization between the free and bound electrons in the high-lying electronic levels.[13] The electron–proton and proton–atomic hydrogen translational energy relaxation times are estimated to be less than the residence times within the expansion nozzle, which is comparable to the hydrogen–molecular nitrogen relaxation time; therefore, Zube and Myers[13] argue that $T_{elec}$ should also reflect the heavy species translational temperature ($T_{tran}$). This is seen to be supported by the model calculations for the comparable power hydrogen arcjet only very near the throat. It is apparent that translational energy exchange is less efficient downstream where $n_e$ drops significantly. It is also apparent from Fig. 2 that $T_{rot}$ and $T_{vib}$ are less than $T_{elec}$ and $T_{trans}$. At first, one may conclude the presence of a substantial departure from local thermodynamic equilibrium for these internal energy modes, as suggested by Zube and Myers.[13] However, we remind the reader that these measurements are based on line-of-sight averages of emission, and so

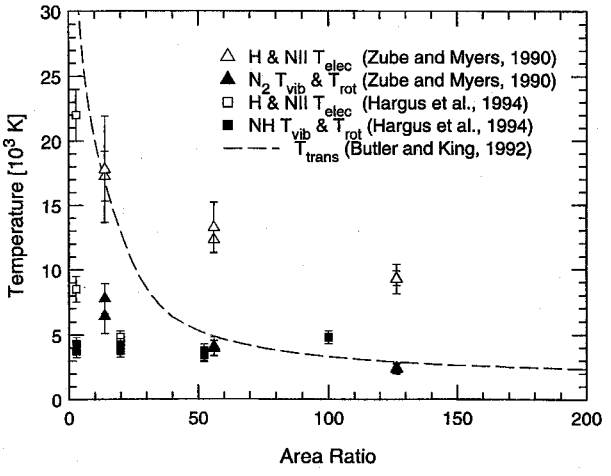


**Fig. 2 Comparison of axial variation in temperatures in the expanding nozzle of a low-power arcjet thruster. The dashed lines are the calculations for a low-power arcjet of Butler[20,23] (see, e.g., Ref. 17) with hydrogen as a propellant. The data points are for a low-power thruster operating on hydrazine decomposition products from Ref. 13 (triangles), and a high-power thruster operating on ammonia from Ref. 14 (squares).**

the signal from any emitting species reflects the local properties in the region where the density of the emitting species is greatest. Because of the high centerline temperatures, it is possible that molecular emission originates from the cooler boundary region within the nozzle and indicates a lower $T_{rot}$ and $T_{vib}$.

The measurements of Zube and Myers[13] were limited to positions 3 mm from the throat of the arcjet. Machining holes closer to the constrictor would be more difficult in such a small device. However, prior to the Zube and Myers study,[13] Ishi and Kuriki[16] successfully modified the constrictor region to accommodate optical access into a low-power arcjet operating on helium propellant. In that study, they positioned optical viewports at four locations within the constrictor, which was 8 mm in length for their design. Their results clearly revealed an internal (constrictor) flow that was far removed from ionizational equilibrium, with the plasma seemingly overdense with respect to Saha equilibrium. The departure from Saha equilibrium was found to be more pronounced farther downstream of the entrance to the constrictor. Although no direct measurements of the departure from ionizational equilibrium have been made in the constrictor or nozzle region of a low-power hydrogen arcjet, it is expected that a similar result would ensue. We would expect that the plasma is near ionization equilibrium in the throat or constrictor, and that the departure from Saha equilibrium would be more pronounced in the diverging region of the nozzle, since electron–atom collisions become less frequent as densities fall.

In an attempt to better understand the constrictor flow region of a 6–12-kW water-cooled hydrogen arcjet, Glocker and Auweter-Kurtz[15] machined optical access into the constrictor, which allowed the imaging of the arc plasma emission onto an intensified charge coupled device (CCD) video camera. Radial profiles of $T_{elec}$ and $T_e$ were obtained from the Abel-inverted intensities of continuum emission (at 600 nm), and relative spectral line emission from the $H_\alpha$ and $H_\beta$ atomic transitions. The measured peak (centerline) temperatures are in agreement, suggesting that the constrictor plasma is in near local thermodynamic equilibrium. However, both methods give peak temperatures in the range of 10,000–13,000 K, which are below their own numerical predictions of approximately 20,000 K,[15] and substantially below the constrictor temperatures predicted in low-power and medium-power radiation-cooled hydrogen arcjets.[17,18] The images captured in Ref. 15 allow for an estimate of the arc diameter within the constrictor. The arc core does not appear to fill the constrictor, and has a diameter that is roughly one-third of that of the constrictor. This result is consistent with the constrictor arc diameter estimated earlier, and that measured in a medium-power, radiation-cooled hydrogen arcjet.[18]

Recent experimental measurements of $n_e$ were made in the near-cathode region of 1- and 5-kW arcjets by Storm and Cappelli.[17,18] No modifications to the prototype arcjets were made, and so these measurements are nonintrusive. Using hydrogen as propellant, the centerline axial emission spectrum was measured and the near-cathode axial line-of-sight (LOS) electron number density was obtained from the Stark broadening of the wings of the $H_\alpha$ line. Radiative transfer effects on the spectral line are localized to near line-center, whereas the linewings are determined by the properties within approximately 1 mm of the cathode tip.[17] The thoriated tungsten cathode temperature was also measured by the broadband emission away from the Balmer lines, accounting for molecular hydrogen and continuum emission, as necessary.

A typical axial emission spectrum in the visible region is shown in Fig. 3. The broadband background is a combination of thermal radiation from the cathode and continuum emission from the plasma electrons. Molecular hydrogen emission was negligible because of the use of very slow optics.[18] Using axial variations of $n_e$ and $T_e$ that were computed using the single-fluid arcjet model of Butler and King[20] for a 5-kW hydrogen arcjet, the continuum emission in the axial direction was calculated with a one-dimensional radiation transfer model. This continuum emission is shown for comparison (dashed line) in Fig. 3. The background continuum is well approximated by the cathode and continuum emission assuming a $T_{cat}$ of 3730 K. In this manner, $T_{cat}$ was varied in the model so as to reproduce the measured continuum emission over a range of $P/\dot{m}$ values, and the results, shown in Fig. 4, indicate that $T_{cat}$ is very near or above the melting point of pure tungsten (3690 K) and increases with $P/\dot{m}$. These results are consistent with well-documented cathode erosion measurements that infer the presence of a molten pool of tungsten at the cathode tip.[25] The increase in $T_{cat}$ with $P/\dot{m}$ predicts an increase in arc current density at the arc attachment, consistent with the measured increase in conductivity, or $n_e$, as discussed next. Note that when the electron number densities computed by the model are artificially increased by about a factor of 3, the measured spectrum agree very well with that simulated on the basis of the other computed variables (dotted line in Fig. 3).

For comparison, Zhou et al.[26] measured the temperatures of thoriated tungsten cathodes in a stationary argon discharge using both single- and two-color pyrometry. They recorded tip temperatures between 3500–3800 K, depending on the cathode diameter and increasing with arc current, and hence, $P$.

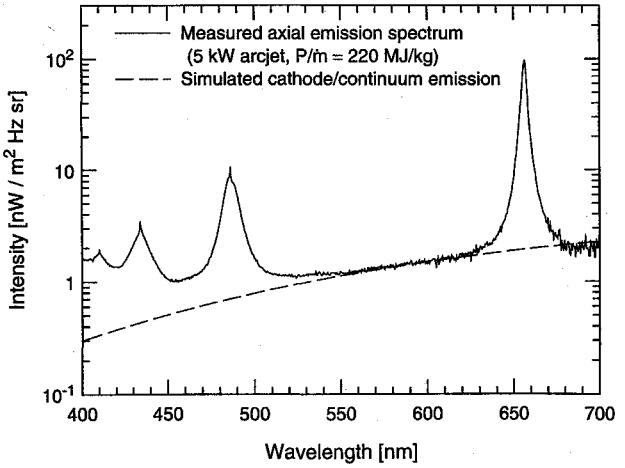


**Fig. 3 Axial emission spectrum of a 5-kW hydrogen arcjet (solid line) and the calculated cathode/continuum emission (dashed line) corresponding to a cathode temperature of 3730 K.**

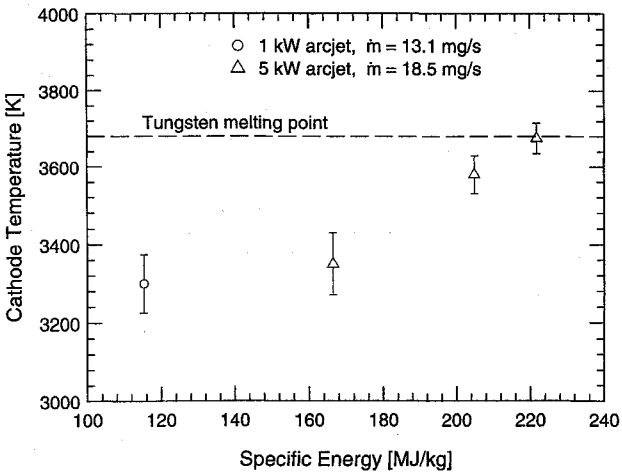


**Fig. 4 Measured cathode temperature in 1- (circles) and 5-kW (triangles) arcjets operating on hydrogen propellant.**

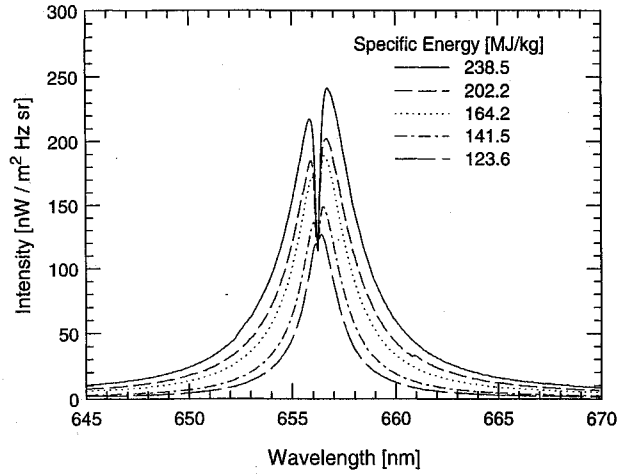


**Fig. 5 Axial emission spectra of the $H_\alpha$ line at various specific energy for the 5-kW hydrogen arcjet showing the blue-shifted reabsorption dip near line center.**

Although these experiments were performed at much higher currents, the current densities are comparable to those in the hydrogen arcjets, and the cathode temperatures are in good agreement with those measured in the arcjet.

Storm and Cappelli[17,18] measured the near-cathode $n_e$ by the Stark broadening of the linewings of the $H_\alpha$ line. Their analysis is limited to the far wings of the line because the line core is expected to experience significant distortion because of self-absorption. Sample $H_\alpha$ emission spectra from the 5-kW arcjet are shown in Fig. 5. The line is broadened considerably because of the large $n_e$ upstream of the constrictor, and the central dip is caused by reabsorption by the relatively cool plasma in the downstream expansion region and plume.[17,18] Based on the relative Doppler shift between the emitting plasma near the constrictor and the absorbing plasma in the plume, one would expect the central dip to be red-shifted by a small fraction of the width of the linewings, if, in accordance with the linear Stark theory, the hydrogen lines are unshifted and symmetric. However, the exact opposite is observed in Fig. 5. The large blue-shift in the central dip can be accounted for by the asymmetry in the Stark broadening of $H_\alpha$, which results in an apparent red-shift of the line at large $n_e$.[27] For $n_e = 2 \times 10^{23}$ m$^{-3}$, a typical value near the cathode (see Fig. 1), the asymmetric Stark red-shift of $H_\alpha$ linewings is approximately 0.12 nm, which is large compared to a Doppler blue-shift of approximately 0.03 nm. Unfortunately, because of the relatively small size of the Doppler shift and the uncertainty in determining the precise spectral line center, the axial velocity in the constrictor region could not be determined.

The width of the linewings, however, could be measured accurately, and from the Stark-broadened fullwidth at half-maximum (FWHM), the near-cathode region $n_e$ was determined.[18] Most previous measurements involving Stark broadening of the Balmer lines of hydrogen (including Ref. 17) have made use of the Stark broadening tables compiled by Vidal, Cooper, and Smith (VCS)[28] in the early 1970s, which assumed perturbations to the atomic energy levels by electron collisions while the ions remained static. Recent Monte Carlo simulations by Kelleher et al.,[29] taking into account dynamic ions, have shown that the VCS tables underpredict the linewidths of $H_\alpha$ by a factor of approximately 2 at electron densities typical of the near-cathode region, and as much as a factor of 30 at lower densities. Use of the VCS tables would then result in greatly overestimated $n_e$ from $H_\alpha$. The present $n_e$ measurements were made using the recent Monte Carlo simulations, whose FWHMs are compared to those of the VCS tables in Fig. 6. However, as these simulations were only performed up to $n_e = 10^{23}$ m$^{-3}$, electron densities larger than this were obtained by extrapolation.

The measured near-cathode $n_e$ for the 1- and 5-kW arcjets are shown as a function of $P/\dot{m}$ in Fig. 7. The 1-kW results differ from those of Ref. 17 because of the improved Stark broadening calculations and linewing fits. The relatively large

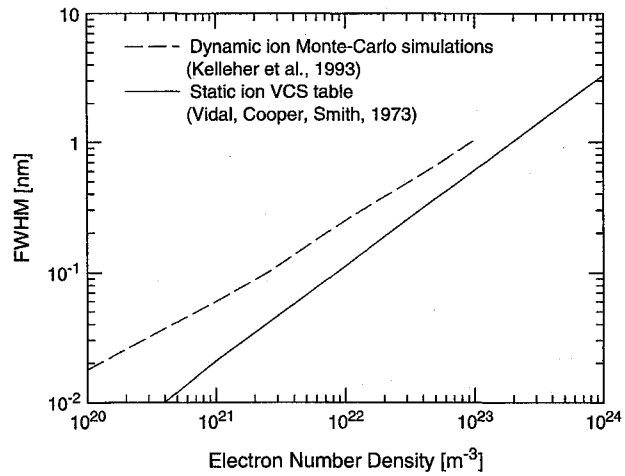


**Fig. 6 Stark broadened FWHM for $H_\alpha$ showing the discrepancy between the computations by VCS[28] and the recent Monte Carlo simulations.**

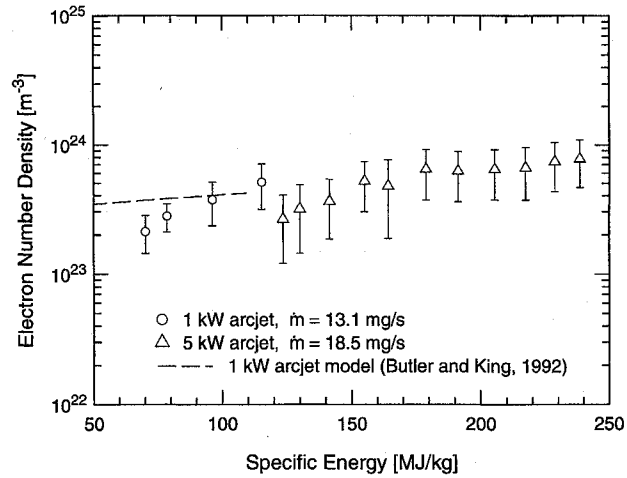


**Fig. 7 Measured near-cathode $n_e$ in the 1- (circles) and 5-kW (triangles) arcjets, compared to the MHD 1-kW arcjet model of Butler and King[20,23] (see, e.g., Ref. 17) (dashed line).**

uncertainties in these measurements are primarily because of the uncertainty in determining precisely which parts of the spectra of Fig. 5 constitute the linewings. In other words, the uncertainty reflects the very nature of these measurements being axial LOS averages within approximately 1 mm of the cathode tip. Nevertheless, despite the large uncertainties, the increase in $n_e$, and therefore, plasma conductivity, with $P$ is apparent. This is consistent with the measured increase in $T_{cat}$ with $P$. Furthermore, the results for the 1-kW arcjet display reasonably good agreement to peak near-cathode $n_e$ predicted by the MHD arcjet model simulations by Butler and King[20,23] (e.g., Ref. 18). The measured densities are somewhat lower than the calculated peak densities because of the fact that they are LOS averages over a small region.

## V. LIF Measurements of Velocity

The first measurements of flow velocity in the nozzle interior were recently made using laser-induced fluorescence by Storm and Cappelli.[19] In that study, axial velocity components in a 1-kW hydrogen arcjet were measured from the Doppler shift of the hydrogen Balmer-$\alpha$ line from an unshifted stationary reference. To obtain optical access to the nozzle interior, the laser excitation beam was directed into the arcjet axially, while the fluorescence was collected broadband at an angle of 16 deg to the arcjet centerline. Since this angle was smaller than the 20-deg divergence half-angle of the nozzle expansion, the plasma could be probed everywhere downstream of the arcjet throat. The drawback to this technique, however, was the considerable background signal created by scattered laser light in the nozzle. This signal noise was the limiting factor in restricting the physical domain of the measurements to near the arcjet centerline where the LIF signal was the greatest. Despite this background noise, measurements were obtained along the axis of the nozzle from the exit plane to within 1.5 mm of the throat, and radial scans were obtained at three different axial positions.

The measured axial velocities are given in Figs. 8 and 9. As no other measurements of velocity have been made in the arcjet nozzle interior, the results can only be compared to simulations of the 1-kW hydrogen arcjet using the model of Butler and King.[20,23] The most recent model results of the centerline axial velocity, given as a function of area ratio in Fig. 8, are in very good agreement with the measurements. The centerline velocity is seen to drop monotonically from a peak of approximately 17.5 km/s at 1.3 mm downstream of the throat (area ratio of approximately 6) to around 12 km/s at the exit plane (area ratio of 225). This apparent axial drop in velocity is contrary to what one would expect in a supersonic diverging

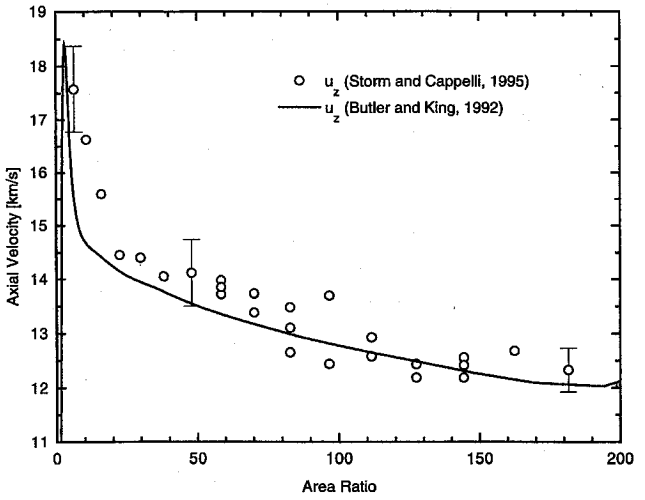


**Fig. 8 Measured axial velocity along the arcjet centerline, compared to the MHD 1-kW arcjet mode of Butler and King[20,23] (see also Ref. 19). Typical errors are shown.**

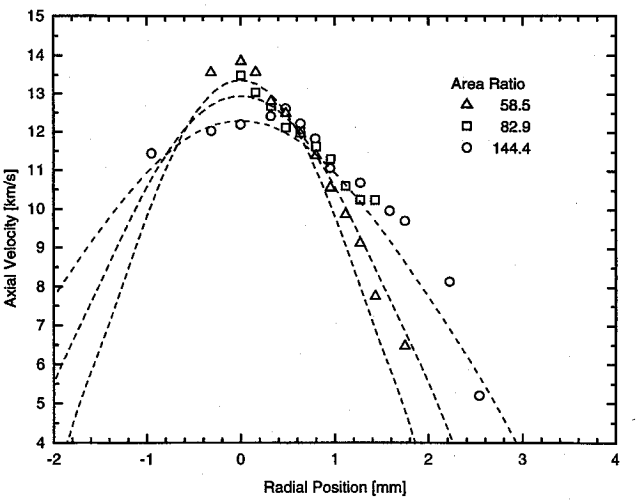


**Fig. 9 Radial profiles of axial velocity at three axial locations within the arcjet nozzle. The errors are typically ±0.6 km/s. The dashed lines are results of the Butler and King[20,23] arcjet model (Ref. 19) at the same axial locations as the measurements.**

nozzle; however, as the centerline temperature drops rapidly in the axial direction (Fig. 2), the Mach number increases as expected. Since the expansion converts thermal energy into kinetic energy, the mass-average velocity must necessarily increase in the downstream axial direction. The observed drop in centerline velocity must therefore be a result of viscous transport of axial momentum in the radial direction, indicating the importance of viscosity in this flowfield.

As a result of the radial transport of momentum away from the nozzle centerline, the axial velocity far from the centerline should increase with downstream position. This is evident in Fig. 9, which shows radial profiles of the axial velocity measured at three axial positions within the nozzle. (The LIF signal intensity drops off quickly with radial position, indicating a rapid radial decrease in the $n = 2$ excited state number density of atomic hydrogen. This loss in signal restricted the measurement domain to within approximately 2 mm of the nozzle centerline.) The dashed lines in the figure are the model results at the same axial locations as the measurements. The measurements and the model show remarkably good agreement, however, the modeled velocities are somewhat lower than the measurements away from the arcjet centerline. As predicted, the velocities away from the centerline increase with axially position. Since most of the mass convection occurs in this outer region, the total kinetic energy of the flow is increasing downstream, as expected.

## VI. Summary

In this article, we have reviewed past measurements of flow properties in the nozzle interior and constrictor (near-cathode) region of arcjet thrusters. Many of the measurements reveal flow behavior that is consistent with recent arcjet simulations. These measurements include static pressure, anode current distribution, plasma density, velocity and temperatures, and cathode temperature. Advances have been made in the use of nonintrusive optical diagnostics to measure arcjet flow properties in the near-cathode and anode throat region, where the arc is greatly constricted and strongly contributes to heat transfer and device performance.

Static pressure measurements in low power arcjets indicate that the sonic point is very near the constrictor, in contrast to similar measurements in higher-power arcjets, where higher aspect-ratio constrictors give rise to boundary-layer growth that moves the sonic point downstream of the constrictor exit. Electron number densities based on static pressure measurements compare favorably to those computed on the basis of resistive MHD simulations. Optical emission measurements in-

dicate that $n_e$ drops downstream of the throat, suggesting a concomitant decrease in the current densities. It is suspected that the drop in current density strongly favors diffuse attachment along the anode.

Electrical measurements using a segmented anode configuration support the notion that the anode arc attachment is diffuse as opposed to constricted. In low-power arcjets, the current appears to be distributed across the anode in a way that is consistent with the observed decrease in plasma density (and, hence, plasma conductivity). Measurements of floating potential permit an estimate of the electric field strength in the throat. From this, we have estimated the extent of arc constriction and have found that the arc cross-sectional area is approximately one-tenth of the constrictor area, consistent with recent estimates based on Stark-broadened axial line emission. It is also apparent, from floating potential measurements, that the anode fall voltage varies dramatically along the anode, being near zero in the region of attachment near the exit plane and close to 40 V at the attachment near the throat.

A range of spectroscopic studies, implemented by collecting plasma emission side-on through holes in the anode, and end on by collecting light axially, support the conjecture that the nozzle flow is removed from thermal equilibrium. The departure from thermal equilibrium is evidenced by an elevated $T_{elec}$, and is less severe in the upstream plasma near the throat. This is expected, since the higher pressures and plasma densities in that region give rise to a plasma that is close to Saha equilibrium. The expansion process creates an overdense plasma and subsequently overpopulates excited electronic levels.

Near-cathode electron number densities are found to be only weakly dependent on $P/\dot{m}$. This trend is captured by the MHD simulations. An increase in static pressure is therefore expected to reflect an increase in throat temperatures, a result that has yet to be verified by experimental observations. For the first time, direct and nonintrusive measurements of $T_{cat}$ have been made in 1- and 5-kW hydrogen arcjet thrusters. These measurements indicate that cathode temperatures apparently exceed the melting point of tungsten at modest $P/\dot{m}$ (200 MJ/kg) and are apparently below the melting point at lower $P/\dot{m}$.

Measurement of plasma velocities in the nozzle expansion flowfield indicate a viscous diffusion of axial momentum away from the arcjet axis and a corresponding decrease in axial velocity. This observation is also seen in the MHD simulations and is an indication of the highly viscous nature of the plasma flow within the arcjet nozzle.

Despite the progress that has been made in diagnostics of the internal flow, many issues related to performance efficiency and lifetime are still unresolved. Although existing models do well at predicting the exit plane plasma conditions, they seem to still overpredict thrust efficiency. It is the combined effort of modeling and experimental measurements of internal flow properties that will lead to a better understanding of plasma flow behavior, and hence, models with better predictive capabilities.

## Acknowledgments

This work was supported in part by the U.S. Air Force Office for Scientific Research, Olin Aerospace Company (formerly Rocket Research Company), and by the NASA Lewis Research Center. Part of the data was obtained while the authors were Visiting Scientists at the NASA Lewis Research Center. The many stimulating discussions with scientists there are gratefully acknowledged.

## References

[1]Vaughan, C., and Cassady, J., "An Updated Assessment of Electric Propulsion Technology for Near-Earth Space Missions," AIAA Paper 92-3202, July 1992.

[2]Manzella, D. H., Curran, F. M., Myers, R. M., and Zube, D. M., "Preliminary Plume Characteristics of an Arcjet Thruster," AIAA Paper 90-2645, July 1990.

[3]Hoskins, W. A., Kull, A. E., and Butler, G. W., "Measurement of Population and Temperature Profiles in an Arcjet Plume," AIAA Paper 92-3240, July 1992.

[4]Carney, L. M., and Keith, T. G., "Langmuir Probe Measurements of an Arcjet Exhaust," *Journal of Propulsion and Power*, Vol. 5, No. 3, 1989, pp. 287–294.

[5]Van Camp, W. M., Esker, D. W., Checkley, R. J., Duke, W. G., Kroutil, J. C., Merrifield, S. E., and Williamson, R. A., "Study of Arcjet Propulsion Devices," NASA CR-54691, March 1966.

[6]Cappelli, M. A., Hanson, R. K., Liebeskind, J. G., and Manzella, D. H., "Optical Diagnostics of a Low Power Hydrogen Arcjet," 22nd International Electric Propulsion Conf., Paper 91-091, Oct. 1991.

[7]Liebeskind, J. G., Hanson, R. K., and Cappelli, M. A., "Flow Diagnostics of an Arcjet Using Laser-Induced Fluorescence," AIAA Paper 92-3243, July 1992.

[8]Beattie, D. R., and Cappelli, M. A., "Raman Scattering Measurements of Molecular Hydrogen in an Arcjet Thruster Plume," AIAA Paper 95-1956, June 1995.

[9]Crofton, M. W., Welle, R. P., Jansen, S., and Cohen, R. B., "Temperature, Velocity and Density Studies in the 1-kW Ammonia Arcjet Plume by LIF," AIAA Paper 92-3242, July 1992.

[10]Talley, K., Elrod, W., and Curran, F. M., "Static Pressure Measurements of the NASA Lewis 1.2-kW Arcjet," AIAA Paper 92-3111, July 1992.

[11]Harris, W. J., O'Hair, E. A., Hatfield, L. L., Kristiansen, M., and Grimes, M. D., "Static Pressure Measurements in a 30-kWe Class Arcjet," AIAA Paper 91-2457, June 1991.

[12]Curran, F. M., and Manzella, D. H., "The Effect of Electrode Configuration on Arcjet Performance," NASA TM 102346, July 1989.

[13]Zube, D. M., and Myers, R. M., "Thermal Nonequilibrium in a Low Power Arcjet Nozzle," *Journal of Propulsion and Power*, Vol. 9, No. 4, 1993, pp. 545–552.

[14]Hargus, W., Micci, M., and Spores, R., "Interior Spectroscopic Investigation of the Propellant Energy Modes in an Arcjet Nozzle," AIAA Paper 94-3302, June 1994.

[15]Glocker, B., and Auweter-Kurtz, M., "Numerical and Experimental Constrictor Flow Analysis of a 10 kW Thermal Arcjet," AIAA Paper 92-3835, July 1992.

[16]Ishi, M., and Kuriki, K., "Optical and Analytical Studies of Arc Column in DC Arcjet," AIAA Paper 87-1086, May 1987.

[17]Storm, P. V., and Cappelli, M. A., "Axial Emission Diagnostics of a Low Power Hydrogen Arcjet Thruster," 23rd International Electric Propulsion Conf., Paper 93-219, Sept. 1993.

[18]Storm, P. V., and Cappelli, M. A., "Axial Emission Measurements on a Medium Power Hydrogen Arcjet Thruster," AIAA Paper 94-2743, June 1994.

[19]Storm, P. V., and Cappelli, M. A., "Laser-Induced Fluorescence Measurements Within an Arcjet Thruster Nozzle," AIAA Paper 95-2381, July 1995.

[20]Butler, G. W., and King, D. Q., "Single and Two Fluid Simulations of Arcjet Performance," AIAA Paper 92-3104, July 1992.

[21]Yuan, B. P., and Cappelli, M. A., "Linear Stability Analysis of the Ionization Layer of a Diffuse Anode Arc," AIAA Paper 95-3064, July 1995.

[22]Yuan, B. P., and Cappelli, M. A., "Stability of a Near-Thermal Plasma in Contact with an Anode," AIAA Paper 95-1991, June 1995.

[23]King, D. Q., and Butler, G. W., "Modeling and Measurements of $N_2$ Arcjet Performance," AIAA Paper 90-2616, July 1990.

[24]Mitchner, M., and Kruger, C. H., Jr., *Partially Ionized Gases*, Wiley, New York, 1974.

[25]Curran, F. M., Haag, T. W., and Raquet, J. F., "Arcjet Cathode Phenomenon," NASA TM 102099, May 1989.

[26]Zhou, X., Berns, D., and Heberlein, J., "Arc Electrode Interaction Study," NASA Grant NAG3-1332, Final Rept. June 1994.

[27]Wiese, W. L., Kelleher, D. E., and Paquette, D. R., "Detailed Study of the Stark Broadening of Balmer Lines in a High-Density Plasma," *Physical Review A: General Physics*, Vol. 6, No. 3, 1972, pp. 1132–1153.

[28]Vidal, C. R., Cooper, J., and Smith, E. W., "Hydrogen Stark Broadening Tables," *Astrophysical Journal Supplement Series*, Vol. 25, No. 214, 1973, pp. 37–136.

[29]Kelleher, D. E., Wiese, W. L., Helbig, V., Greene, R. L., and Oza, D. H., "Advances in Plasma Broadening of Atomic Hydrogen," *Physica Scripta*, Vol. T47, 1993, pp. 75–79.